ACS OMEGA

http://pubs.acs.org/journal/acsodf

Article

Electrochemically Induced Mesomorphism Switching in a Chlorpromazine Hydrochloride Lyotropic Liquid Crystal

Robert D. Crapnell, Huda S. Alhasan, Lee I. Partington, Yan Zhou, Ziauddin Ahmed, Amal A. Altalhi, Thomas S. Varley, Nadiyah Alahmadi, Georg H. Mehl, Stephen M. Kelly, Nathan S. Lawrence, Frank Marken, and Jay D. Wadhawan*

Cite This: *ACS Omega* 2021, 6, 4630−4640

Read Online

ACCESS | Metrics & More | Article Recommendations

ABSTRACT: The discovery of electrochemical switching of the L_α phase of chlorpromazine hydrochloride in water is reported. The phase is characterized using polarizing microscopy, X-ray scattering, rheological measurements, and microelectrode voltammetry. Fast, heterogeneous oxidation of the lyotropic liquid crystal is shown to cause a phase change resulting from the disordering of the structural order in a stepwise process. The underlying molecular dynamics is considered to be a cooperative effect of both increasing electrostatic interactions and an unfolding of the monomers from "butterfly"-shaped in the reduced form to planar in the oxidized form.

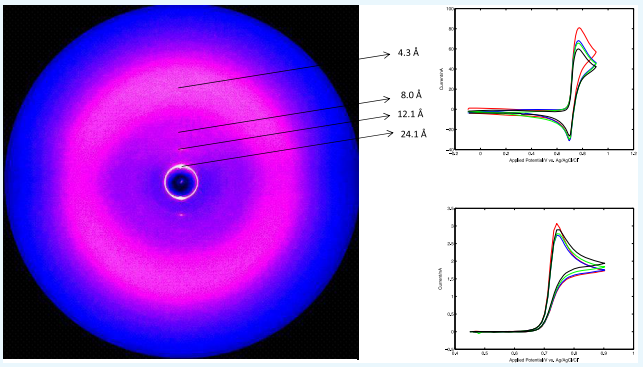

INTRODUCTION

Conformational changes in redox-active molecules can be triggered electrochemically.[1] Such changes do not always have to occur simultaneously with heterogeneous electron transfer; they can both precede, or follow from, the electron transfer event[2] so that voltammetry can identify intermediates and evaluate their lifetimes. One of the characteristics of conformational change occurring in concert with electron transfer is sluggish electrode kinetics, since this can affect the reorganization energy for the heterogeneous electron transfer,[3] as seen for the reduction of cyclooctatetraene[1,3,4] and some of its derivatives[1] and nitrogen analogues,[1,5] wherein a nonplanar, "tub"-shaped neutral molecule affords a planar anion radical.[1,3−5] A second, more important, feature is due to the fact that any intermediate state does not last more than a few vibrations[6] so that the observation is that there is a complete absence of an intermediate, even at the fastest, nanosecond timescales (corresponding to a few million volts per second scan rates) that can be explored voltammetrically.[7,8] Complications in the following conformation change resulting from heterogeneous electron transfer include ion pairing[1] and potential inversions for two-electron transfers.[9] In this article, following reports of electron transfer-induced mesomorphism in thermotropic liquid crystals based on ferrocene derivatives,[10−12] and in nickel(II)-based mesogenic systems,[13] we investigate whether the mechanism of electrochemically trigged conformational change can change as a result of close-packing monomers within a self-assembled, redox-active, liquid nanosystem (viz., lyotropic liquid crystal) based on chlorpromazine hydrochloride.

The tranquilizing drug, chlorpromazine (Figure 1a), and its derivatives are often used as one-electron mediators in electrochemistry,[14] as well as in the treatment of schizophrenia;[15] its biological activity is thought to derive from its facile oxidation and photo-oxidation to a stable cation radical[16−40] and its flexibility:[31−37] in the solid state and in solution, the neutral molecule folds about the N−S axis with the central six-ring in a boat confirmation ("butterfly"-shaped, dihedral angle of 139−153°, Figure 1a), with rapid molecular motions that include those associated with the side chain, pyramidal inversion at nitrogen and ring inversion, even at low temperatures.[35] Oxidation to the cation radical flattens the ring system through relaxing steric repulsions and readjusting the side chain,[33] so that the dihedral angle opens up to 170−180°.[31−37] In contrast, further oxidation to the dication followed by hydrolysis with water yields the corresponding sulfoxide, which is thought to exist with the central six-ring in the boat conformation, at least in the solid state.[36] Accordingly,

Received: October 29, 2020
Accepted: December 18, 2020
Published: February 5, 2021

(a)

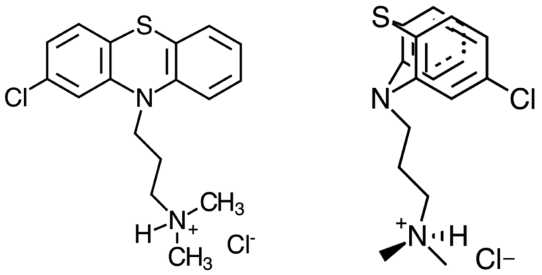

(b)

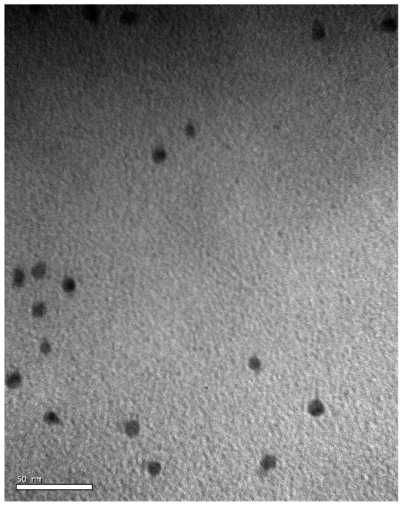

Figure 1. (a) Structure of chlorpromazine hydrochloride in planar (left) and quasi-equatorial (right) conformations. The latter has been drawn to emphasize the boat conformation of the central six-ring. (b) Transmission electron micrograph of chlorpromazine hydrochloride aggregates obtained in an aqueous solution comprising 13.1 mM chlorpromazine hydrochloride and 36.0 mM zinc chloride. The scale bar corresponds to 50 nm.

the conformational change on oxidation to the cation radical affords a bathochromic shift in the absorption: slightly yellow chlorpromazine[24,25,41] (white as the hydrochloride on the side chain,[21,38,41] pK_{BH^+} = 9.15−9.3) converts to the pink cation radical[22,38] (λ_{max} = 526−534, 775−865 nm); the sulfoxide is known to be red.[22] Chlorpromazine is a surfactant,[42−56] affording "cup-stack" micelles[54] (where the hydrophobic core comprises the aromatic rings, with the alkyl chains penetrating into the aqueous pseudophase, enabling the formation of a micellar palisade layer), with a critical micelle concentration (cmc) that depends on the ionic strength, electrolyte nature and temperature of the aqueous solution:[42,43,46−52,55] it ranges between 21 and 27 mM at ambient temperature in water, decreasing to between 2 and 8 mM (aggregation number between 6 and 40) in the presence of 0.1 M NaCl. It is notable that even at concentrations two orders lower than the cmc, self-association of chlorpromazine can occur.[45] Indeed, we have been able to observe aggregates (7.5 ± 2.0 nm radius, assumed spherical, Figure 1b) in an aqueous solution containing 13.1 mM chlorpromazine hydrochloride and 36.0 mM zinc chloride (corresponding to an ionic strength of ca. 0.1 M), roughly in agreement with cmc aggregation numbers for micelles in which the hydrophobic core is a stacked bilayer of aromatic rings:[54] treating chlorpromazine hydrochloride as having planar dimensions of 1 nm × 1 nm, with 0.33 nm interplanar distance between monomers,[54] and assuming the aggregates illustrated in Figure 1b as having a longest length of 15 nm, the monolayer aggregation number n can be estimated from the relationship: $n(1\text{ nm}) + (n-1)(0.33\text{ nm}) = 15\text{ nm}$, yielding $n \sim 10$, and thus a micelle aggregation number, $N \sim 20$ for a bilayer system. This is in agreement with experimental estimates[42,43,49,51] of between 12 and 40 for chlorpromazine hydrochloride at the cmc (8 mM for 0.1 M NaCl). Surprisingly, however, lyotropic liquid crystals of chlorpromazine in water have never been reported. Accordingly, we first examine the electrochemical switching behavior of chlorpromazine hydrochloride in dilute solution, and subsequently investigate both structural and electrochemical effects within its lyotropic liquid crystalline phase.

RESULTS AND DISCUSSION

One-electron voltammetric oxidation of chlorpromazine (in aqueous 0.1 M KCl) yields the cation radical (Figure 2a). In the absence of nucleophiles or electron donors,[18−22,57−66] this species is considered to be stable in solution (decaying in unbuffered water at pH 7 with a first-order rate constant of $2.9 \times 10^{-3}\ s^{-1}$ at ambient temperature).[19] As evidenced in Figure 2b, the electron transfer is Nernstian at low scan rates (<100 mV s^{-1}), where the peak oxidation (E_p^{Ox}) and reduction (E_p^{Red}) potentials become independent of the voltammetric timescale. The second oxidation to afford the dication (not shown) occurs typically at ca. 400 mV greater potentials. At chlorpromazine concentrations below (or near) the cmc, the peak-to-peak potential difference (ΔE_{pp}) also indicates slight deviation from electrochemical reversibility (75.8 ± 10.6 mV), this changes to electrochemical quasi-reversibility above the cmc (ΔE_{pp} = 97.6 ± 13.8 mV). Curiously, the oxidative peak potential shifts positively by 24.4 mV/decadic change in chlorpromazine concentration, whilst the reverse peak moves only by 11.9 mV/decade. This has the effect of making the oxidation process more difficult as the degree of aggregation increases, with $E_{mid} = {}^1/_2(E_p^{Ox} + E_p^{Red})$ varying by 18.2 mV/decade. This is in agreement with literature studies on the influence of self-assembly on redox properties.[65−68] Accordingly, we suggest this reflects the additional energy required to separate aggregated molecules, owing to both the increased charge and the "butterfly-shaped"-to-planar transition that occurs on oxidation, which is manifested through an intrinsic activation barrier.[6] Given that ring inversion in dilute solutions of chlorpromazine is considered to be rapid, even at low temperature,[35,54] we thus suggest that these data are consistent with conformational change occurring in concert with electron transfer.

The growth of the aggregates to afford micelles and then larger micelles can be inferred from the voltammetric data in Figure 2a,[69] through the extraction of the diffusion coefficient (D) from Randles−Ševčík plots illustrating the variation of the peak oxidative current (i_p^{Ox}, from the first cycle) with scan rate (v), using the equation $i_p^{Ox} = 0.443FSc_0\sqrt{D}\sqrt{\frac{Fv}{RT}}$ where F is the Faraday constant (96 485.3 C mol^{-1}), S is the geometric area of the working electrode, T is the absolute temperature, and R is the molar gas constant (8.3145 J mol^{-1} K^{-1}). As indicated in Figure 2c, the diffusion coefficient decreases with increasing chlorpromazine concentration, even when corrected for the increased viscosity of the solution.[70] Note that the data reported in Figure 2c were also extracted from peak oxidation currents from cyclic voltammograms in aqueous acetate buffer at pH 4, and through Levich plots of the limiting current of

https://dx.doi.org/10.1021/acsomega.0c05284
ACS Omega 2021, 6, 4630−4640

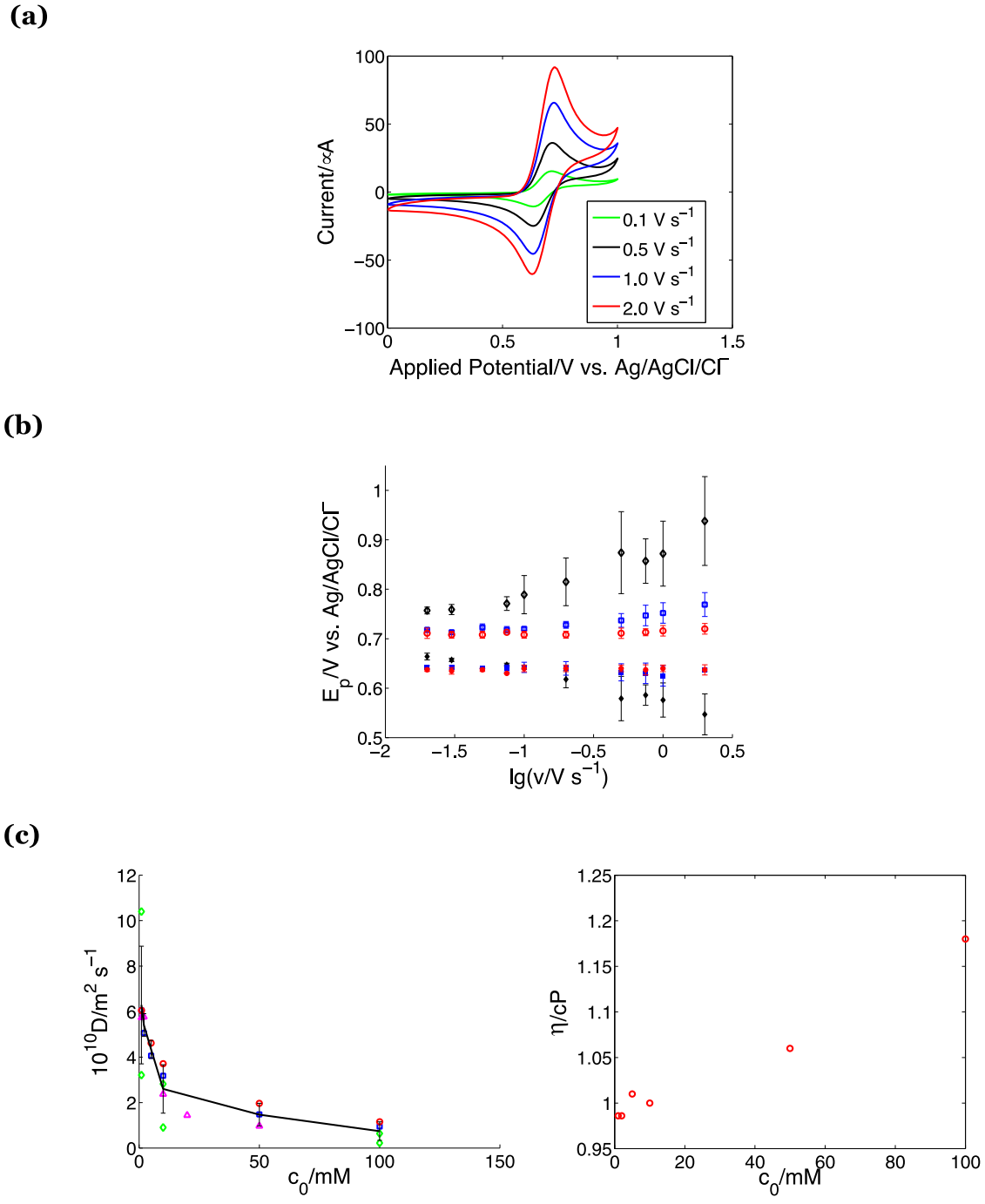

Figure 2. (a) Cyclic voltammograms (fourth scan from a series of four cycles illustrated) for the oxidation of 1.0 mM chlorpromazine hydrochloride in aqueous 0.1 M aqueous potassium chloride solution, recorded using a 3.0 mm diameter glassy carbon working electrode swept at a rate of 0.1 V s^{-1} (green), 0.5 V s^{-1} (black), 1.0 V s^{-1} (blue), and 2.0 V s^{-1} (red). (b) Variation of the voltammetric peak potentials (from the first scan) with experimental timescale at various concentrations of chlorpromazine hydrochloride: 1.0 mM (red circles), 10 mM (blue squares), 100 mM (black diamonds); open symbols refer to the oxidative peak, with filled symbols corresponding to the re-reductive peak. Data points are plotted as the average over two measurements, with error bars indicating one standard deviation. (c) Variation of the diffusion coefficient, D, (left) and aqueous solution (0.1 M KCl) viscosity, η (right), with chlorpromazine hydrochloride concentration (c_0). For the left panel, the aqueous solution was 0.1 M KCl (green diamonds and blue squares as an internal laboratory repeat), pH 4 acetate buffer with 0.1 M KCl (magenta triangles), from cyclic voltammetric measurements at a 3.0 mm glassy carbon electrode, and 0.1 M KCl using steady-state currents at a 5.5 mm × 4.5 mm platinum channel flow electrode (red circles). The black line is the average of all of the data illustrated, with the error bar representing one standard deviation.

steady-state voltammograms (i_{lim}) obtained at a channel flow electrode against the cube root of the volume flow rate (V_f), over a limited range of volumetric flow rates (5−50 μL s^{-1}). In the latter, diffusion coefficients were determined using the expressions,[71] $i_{lim} = FSc_0k_m$ and $Sh = 1.849\left(Pe\frac{d_e}{x_e}\right)^{1/3}$, where k_m is the average mass transport coefficient, Sh is the Sherwood number, Pe is the Péclet number, d_e is the hydraulic diameter,

https://dx.doi.org/10.1021/acsomega.0c05284
ACS Omega 2021, 6, 4630−4640

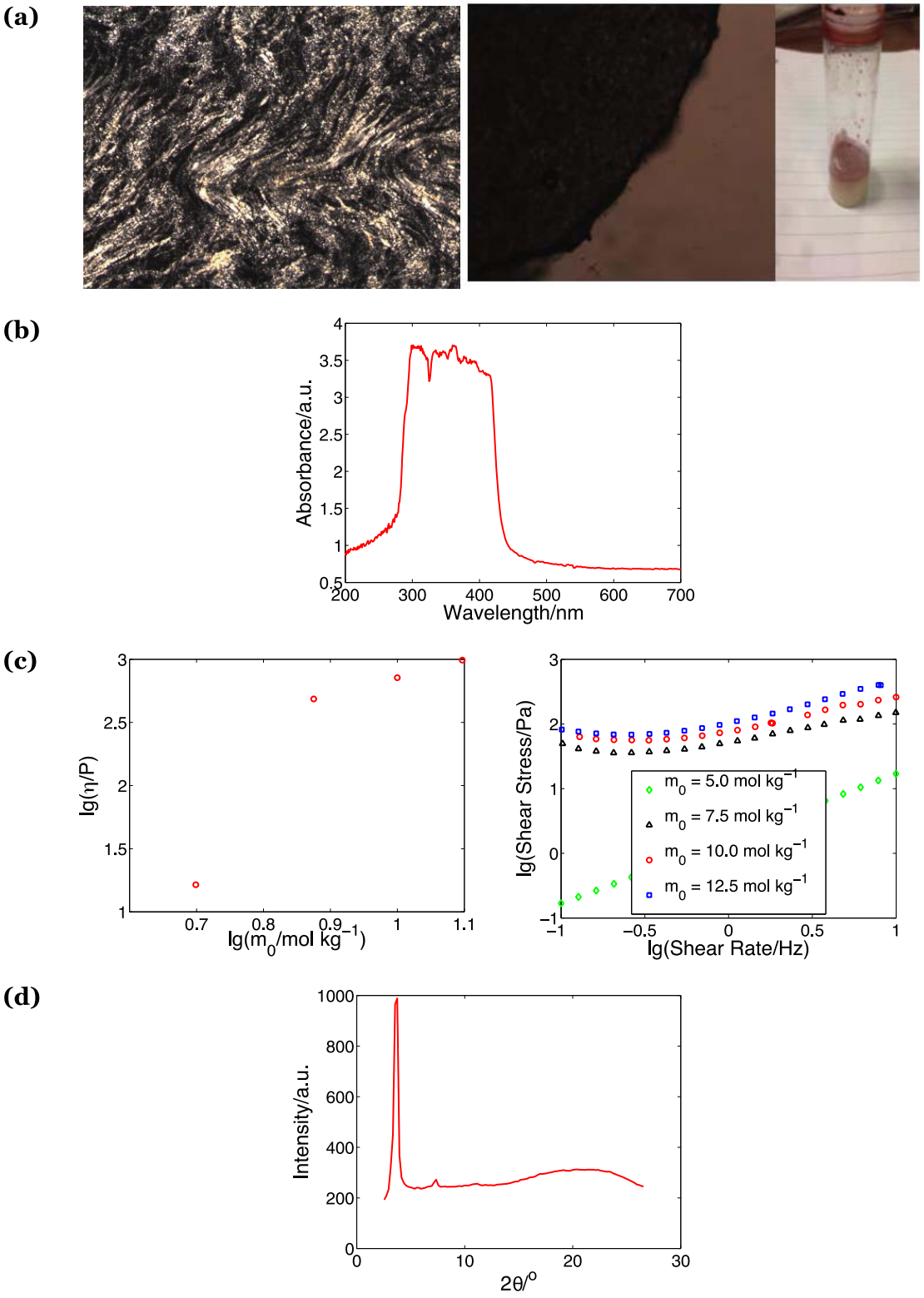

Figure 3. (a) Polarizing microscope images (under crossed-polarizers) of the L_α phase of chlorpromazine hydrochloride in water at 10.0 mol kg^{-1}, freshly prepared (left, magnification × 100) and after 4 months of standing in light and air (middle). Note that in the latter image, a part of the slide outside the cover plate was imaged so as to illustrate the contrast. The image on the right-hand side illustrates the formation of the oxidized material (red-pink) on top of the un-oxidized material (yellow). (b) UV−visible absorption spectrum of the L_α phase of chlorpromazine hydrochloride in water at 10.0 mol kg^{-1}. (c) Rheological properties of the chlorpromazine hydrochloride/water system at various chlorpromazine hydrochloride molalities (m_0): left, viscosity (η) as a function of molality; right, basic shear diagram affording plastic viscosities of 201.2, 306.6, and 499.7 P, and Bingham yields of 30.9, 45.3, and 53.1 Pa for m_0 = 7.5, 10.0, and 12.5 mol kg^{-1}, respectively. (d) X-ray scattering patterns obtained from the L_α phase of chlorpromazine hydrochloride in water at 10.0 mol kg^{-1}. The primary beam is not shown.

https://dx.doi.org/10.1021/acsomega.0c05284
ACS Omega 2021, 6, 4630−4640

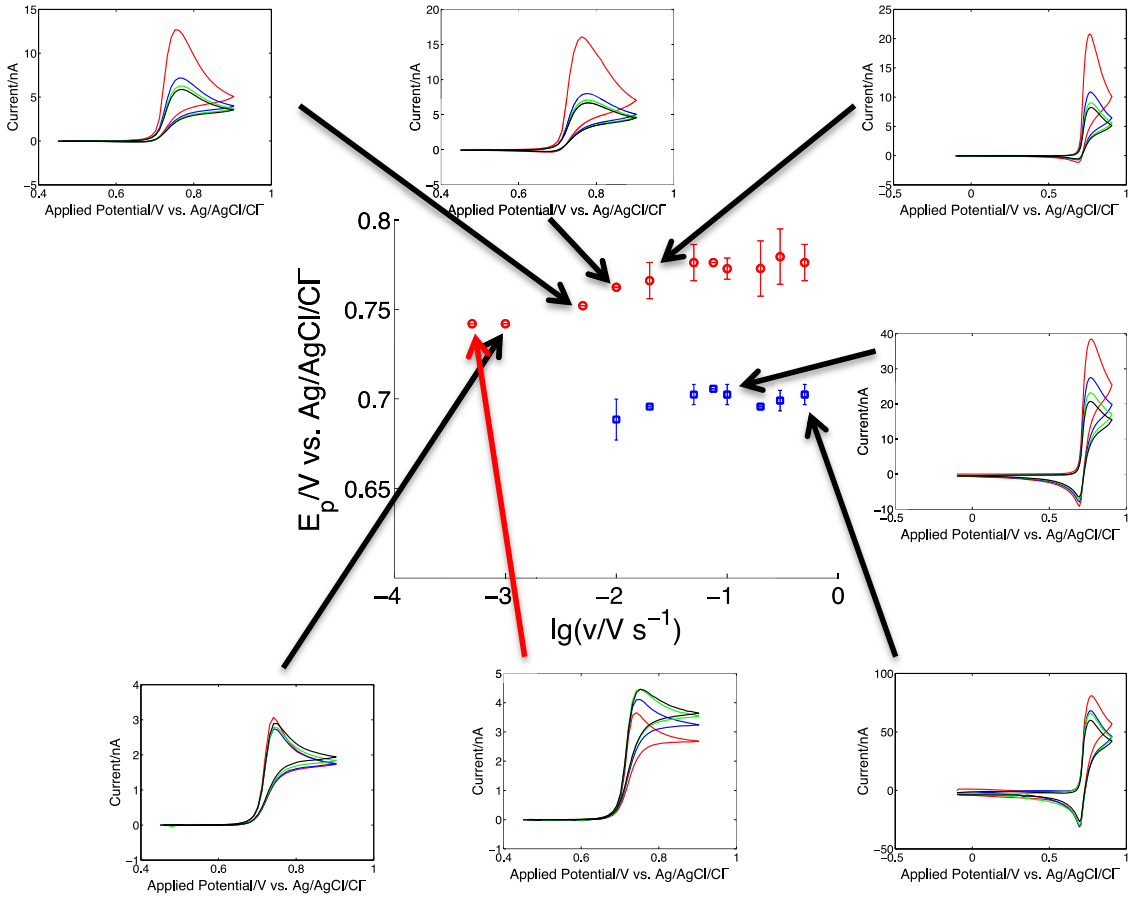

Figure 4. Microelectrode voltammetry of the L_α phase of chlorpromazine hydrochloride in water at 10.0 mol kg^{-1} at an 11 μm diameter carbon microelectrode. The main image is the variation of the peak potentials with experimental timescale (the error bars correspond to one standard deviation), with peripheral images illustrating four consecutive cycles in the voltammetry at 500, 100, 20, 10, 5, 1, and 0.5 mV s^{-1}. In these images, the first cycle is shown in red, with the subsequent cycles being first in blue, then green, and finally black.

and x_e is the electrode length. The data in Figure 2c indicate consistency in the measurements made with different techniques, and suggest a cmc of ca. 10 mM, with self-association of chlorpromazine hydrochloride occurring well below this concentration, in agreement with the literature.[42−54] The continual decrease of diffusion coefficient with increasing chlorpromazine concentration, which is consistent with the notion of increasing micellar size, prompted the investigation as to whether a lyotropic mesophase could be formulated—while *N*-alkyl-phenothiazines have been studied when incorporated into lyotropic liquid crystals,[72] to the best of our knowledge, no lyotropic liquid crystals based on such derivatives have been reported. Here, the idea was to seek to magnify the effect of conformational change through cooperative effects associated with self-assembly into tight liquid nanosystems.[65]

Formulations of 1.0 and 2.0 mol kg^{-1} chlorpromazine in water appeared dark when viewed under crossed-polarizers, indicative of the normal micellar phase; further addition of chlorpromazine to 5.0 mol kg^{-1} yielded transient birefringence and Myelin figures, which on further addition to 10.0 mol kg^{-1}, yielded stable, long-lasting birefringence, even in the presence of mechanical agitation of the phase. Under crossed-polarizers, classical, rough, oily-streak textures were observed (Figure 3a). These are typical of lamellar (L_α) lyotropic liquid crystals. Concurrent with this was the change in the color of the chlorpromazine/water mixture: dilute aqueous solutions are clear and colorless; this changed to a cloudy, pale yellow viscous mixture by 10.0 mol kg^{-1}, with a large absorption band occurring in the violet-to-blue region (300−420 nm, Figure 3b), which is in contrast to the well-defined peaks that occur in dilute solution.[53] The onset of liquid crystallinity in the formulation is marked by the discontinuous increase in the viscosity measured at a constant shear rate of 1.13 Hz between 5.0 and 7.5 mol kg^{-1} (Figure 3c). Indeed, the basic shear diagrams presented in Figure 3c demonstrate Newtonian behavior at 5.0 mol kg^{-1}, with shear thinning, Bingham plastic behavior (plastic viscosities and yield stresses were determined[73] through the fit of shear stress with shear rate in the range 0.2−4 Hz, to yield plastic viscosity >200 P, increasing with molality) for the liquid crystalline material (m_0 > 5.0 mol kg^{-1}), as expected for lamellar (L_α) lyotropic liquid crystals:[74] the shear stress, at high shear rates (>0.2 Hz), increases roughly as a linear function of the shear rate, corresponding to large yield stresses (>30 Pa) which increase with the volume fraction of chloropromazine hydrochloride; this increase gradually tails off at shear rates larger than ca. 4 Hz, as expected.[74] For all three liquid crystal systems examined, there are discontinuities in the flow behavior at low shear rates (<0.2 Hz). This is attributed to "wall slip" where micelles may deplete from the liquid region closest to the surface enabling a thin layer of pure continuous phase to form adjacent to the surface, lowering the viscosity.[75,76] X-ray scattering (Cu K_α radiation at 1.54 Å) was used to characterize the structure of

https://dx.doi.org/10.1021/acsomega.0c05284
ACS Omega 2021, 6, 4630−4640

the L_α phase at 10.0 mol kg^{-1} (Figure 3d), wherein it is seen that, at small angles ($3.65° \leq 2\theta \leq 11.0°$), there are three Bragg spacings (strong first- and second-order reflections, with a very weak third-order reflection) in the ratio 1:1/2:1/3, characteristic of the large separations of the L_α arrangement. The fundamental crystal spacing (d) was determined using the Bragg equation: d (Å) = $1.54/(2 \sin\theta)$, with the scattering vector (q) estimated through $q = 2\pi/d$, so that Bragg ratios q/q_0 could be determined, in which q_0 is the fundamental repeat distance in the lamellar system (viz. center-to-center separation between surfactant aggregates). We calculated a fundamental repeat distance of 2.42 nm, corresponding to the thickness of the surfactant and the water layers. For this 10.0 mol kg^{-1} formulation (78 wt %), the thickness of the individual surfactant layers is estimated as 1.88 nm, which, in the light of X-ray crystallographic data for chlorpromazine hydrochloride, suggests the formation of a surfactant bilayer, as expected. The diffuse peak occurring at the wide angle of $2\theta = 20.3°$, corresponds intra-aggregate spacings (0.44 nm) between the alkyl chains.[54] This tight-packing of the individual monomers suggests that conformational change upon oxidation may disrupt the L_α phase. Indeed, incubation results of the samples in the dark and in the absence of oxygen over a period of four months were observed to be stable and retained their pale yellow coloration; in contrast, samples exposed to both sunlight and oxygen developed a pink-red coloration, which, did not exhibit optical anisotropy when viewed through crossed-polarizers (Figure 3a), indicative of mesomorphism. This is in line with the expectation that flattening the chlorpromazine structure increases the molecular volume of the hydrophobic core, thereby increasing the area of the head group relative to the core through self-distancing of the individual oxidized monomers, and changing the aggregate curvature from zero (L_α) to positive. We did not undertake a chemical analysis of the pink-red material; it is likely that this is a mixture of the cation radical and the sulfoxide.[22,24−30,39,64]

The apparent fast conformational change in oxidation of chlorpromazine in dilute solution, but slow oxidative breakdown of the long-range order in the 10.0 mol kg^{-1} anisotropic phase was next investigated through microelectrode voltammetry (Figure 4) so as to quantify the effective relaxation time. Microelectrodes have the multiple advantages of being sufficiently small in size so that only small amounts of material need to be prepared, whilst providing improvements in signal-to-noise ratio, at steady-state, at reduced Ohmic loss. Since the resistance at a disk electrode of radius r_0 is $\rho/4r_0$, where ρ is the bulk resistivity of the L_α phase (experimentally determined as 46.4 Ω cm), the Ohmic drop is then ca. 2 mV at the highest scan rates used (corresponding to a maximum current flow of ca. 100 nA). It is clear that a single pair of well-defined Nernstian oxidation and reduction signals is observable at high scan rates (ΔE_{pp} = 74 ± 10 mV), corresponding to the oxidation of chlorpromazine to the corresponding cation radical and its re-reduction, with the reverse peak being considerably thinner than the forward, oxidative peak (cf. half-peak widths of ca. 20 mV with 50 mV for the reverse and forward waves, respectively). At higher potentials, typically around 200 mV more positive (at a scan rate of 100 mV s^{-1}) than those illustrated in Figure 4, a second oxidation wave is observable (data not shown) corresponding to the oxidation of the cation radical to the dication. As for the case in dilute, isotropic solution, this second oxidation wave is chemically irreversible, owing to nucleophilic attack by water on the dication.[64]

The quantitative treatment of the voltammograms requires the effective concentration (in moles per unit volume of the phase)[77,78] to be known. The density of the 10.0 mol kg^{-1} L_α phase was determined to be 1.30 ± 0.12 g mL^{-1}, leading to an effective concentration, c_0 of 2.858 ± 0.263 M. The diffusion coefficient was determined as being $(2.0 \pm 0.3) \times 10^{-12}$ m^2 s^{-1} from Randles−Ševčík plots using data from the higher scan rates investigated (≥75 mV s^{-1}). Given the liquid crystalline phase is optically anisotropic, it follows that diffusive transport to the electrode might, likewise, be anisotropic. Surprisingly, however, diffusion within the L_α phase was found to be essentially isotropic, viz. the axial diffusion coefficient (D_z) is not significantly different from the tangential diffusion coefficient (D_r): following previous protocols,[78] and using $D = \sqrt{D_r D_z} = 2.0 \pm 0.3 \times 10^{-12}$ m^2 s^{-1}, the first-cycle oxidative peak currents (i_p^{Ox}) for the high-scan regime were dimensionalized using $\psi_p = \frac{i_p^{Ox}}{4FDr_0c_0} = 0.34\, e^{-0.66a\sqrt{v}} + 0.66 - 0.13\, e^{-11/(a\sqrt{v})} + 0.351a\sqrt{v}$, where $a = \frac{r_0}{\sqrt{D_r}}\sqrt{\frac{F}{RT}}$. A nonlinear least-square fit, using the Levenberg−Marquardt algorithm afforded a good correlation using c_0 = 2.858 M (coefficient of determination, R^2 = 0.9803), with $D_r = (2.5 \pm 0.4) \times 10^{-12}$ m^2 s^{-1} and $D_z = (1.6 \pm 0.7) \times 10^{-12}$ m^2 s^{-1}. We suggest that this apparent transport isotropy arises from the fact that the hydrophobic core is a bilayer of aromatic rings, with the electron lost from the ring nitrogen.[33,64]

The cation radical is less stable in the L_α phase than in aqueous solution—sequential scanning of the voltammetric perturbation reveals the gradual loss of material at higher scan rates. However, on lowering the scan rate, the voltammograms stabilize (cf. the voltammograms at 1 and 500 mV s^{-1} in Figure 4), and exhibit characteristics corresponding to a switch in diffusion regime (from one- to two-dimensional diffusion) at longer timescales,[79,80] with essentially stable scans on repetitive cycling, indicative of chemical reversibility with fast heterogeneous electron transfer. The variation of the one-electron oxidation peak potentials with scan rate, illustrated in Figure 4 is consistent with a first-order transition corresponding to an electrochemically triggered breakdown of the liquid crystal order (mesomorphism), with the voltammograms at the higher scan rates (≥75 mV s^{-1}) typically exhibiting relatively unperturbed, reversible Nernstian waves (peak potentials being independent of scan rate, half-peak widths of 52 ± 5 mV) based around a formal potential of 0.75 ± 0.1 V vs Ag/AgCl/Cl^-, effectively uncomplicated by follow-on kinetics, whilst those at lower scan rates being thinner (40 ± 10 mV), and eventually reversible Nernstian waves centered around a new formal potential 0.71 ± 0.1 V vs Ag/AgCl/Cl^-. At these lower scan rates, the oxidation becomes easier, with the peak shifting by 30 ± 7 mV/decade, and eventually become independent of scan rate. This corresponds to the reversible oxidation of chlorpromazine into an equilibrium mixture ($\lg K$ = 0.45 ± 0.24) of the radical cation in both the L_α phase and the normal micellar solution, with a first-order rate constant for the phase change of 0.70 ± 0.15 s^{-1}, estimated from the KG to DE transition in the reported kinetic zone diagram.[81]

The phase change results in an apparent paradox at very low scan rates—the voltammograms in Figure 4 take on the shape expected for an electrochemically irreversible system, but do

https://dx.doi.org/10.1021/acsomega.0c05284
ACS Omega 2021, 6, 4630−4640

not exhibit decreasing signals upon repetitive cycling. This suggests that, at these slow scan rates (<1.0 mV s^{-1}), there is sufficient time for the electrochemically triggered phase change to be irreversible, giving rise to the observed waveshape. Moreover, under these conditions, the marked *increase* in peak oxidation current and its shift toward more positive potentials is rationalized as being due to an increase in the local viscosity of the system upon mesomorphism. This analysis assumes that there is negligible volume change during the phase transformation driven by both conformational change and electrostatic interactions. Work on the voltammetry of redox liquid microdroplets, which may generate a phase (due to counterion insertion) starting from the triple phase boundary, suggests that such volume changes, even for immiscible phases, tends to either have little effect on the voltammetry or yield subsequent scans with oxidative peaks shifted negatively.[82] The peak shift between the first scan and the stabilized third/fourth scans in the voltammograms recorded at 0.5 mV s^{-1} is 10.1 mV. Although this is comparable with the average error in the recording of the first scan of the voltammograms over several experiments (ca. 8 mV), and neglecting reference potential drift, given the voltammgrams at 1 mV s^{-1} and higher, the peak potential in this region of the EC mechanism is given[83] by $E_p^{Ox} = E^{0''} + \frac{RT}{2F}\ln\left(\frac{D_{Red}}{D_{Ox}}\right) + 1.109\frac{RT}{F}$, where $E^{0''}$ is the formal potential for the oxidation of the system to afford an equilibrium mixture and D_i (i = Red or Ox) is the diffusion coefficient of the reduced and oxidized species. Thus, we find $D_{Red} \sim 3D_{ox}$, indicating that the diffusion coefficient for the cation radical in the disordered, normal micellar solution to be ca. three times smaller than that in the ordered L_α phase. This is roughly in line with expectation, based on the viscosity trends illustrated in Figure 3c, where molecular ordering to form a lamellar phase results in a reduced viscosity than would be expected from the normal isotropic phase. It thus follows that the tightly packed nature of the lyotropic phase enables high rates of electron hopping across bilayer sheets. This is Dahms−Ruff electron hopping, the rate constant for which may be calculated from the diffusion coefficient:[84] $D = \frac{1}{6}k\delta^2 c_0$, where k is the self-exchange rate constant, c_0 is the effective homogeneous concentration, and δ is the thickness of the water layer separating the surfactant pseudophase, determined from X-ray scattering to be 0.54 nm. The isotropic diffusion coefficient suggests a rate constant of ca. 1.5×10^7 M^{-1} s^{-1}, which is reasonably high, whilst the less ordered system is probably limited through translational diffusion through the viscous surfactant system.

CONCLUSIONS

In summary, the amphiphile chlorpromazine hydrochloride (CPZ·HCl) aggregates in dilute solution at concentrations smaller than the cmc; the latter is readily seen through a marked change in the diffusion coefficient with concentration. One-electron oxidation occurs with a conformation change from butterfly to planar shape. Although this unfolding process is electrochemically reversible, it becomes increasingly sluggish with aggregation, indicative of a concerted electron-conformational change. We have discovered that the micelles themselves can aggregate further to form lamellae for the surfactant pseudophase, yielding a lyotropic liquid crystal. Although this phase is optically anisotropic, electron hopping transport within this phase is essentially isotropic. Oxidation breaks down this ordered structure—the oxidized liquid crystal has a half-life of ca. 1.0 s, to yield an isotropic phase (N). This oxidation can be mediated by oxygen and light, or occur heterogeneously at an electrode surface, with fast electrode kinetics consistent with the following mechanism:

$$(CPZ{\cdot}HCl)_{L_\alpha} - e \rightleftarrows (CPZ{\cdot}HCl^{\bullet+})_{L_\alpha}$$

$$(CPZ{\cdot}HCl^{\bullet+})_{L_\alpha} \underset{0.25\ s^{-1}}{\overset{0.7\ s^{-1}}{\rightleftharpoons}} (CPZ{\cdot}HCl^{\bullet+})_N$$

$$(CPZ{\cdot}HCl^{\bullet+})_N + e^- \rightleftarrows (CPZ{\cdot}HCl)_N$$

The underpinning molecular rationale for this stepwise mesomorphism is either due to increased electrostatic interactions that are poorly supported by the counterions, or, more likely, due to the change in space required by the butterfly-to-planar transition. Such phase transitions may find application of these switchable materials for the development of new types of redox sensors, based on polarizing microscopy or electrochemical techniques.

EXPERIMENTAL SECTION

All chemical reagents were purchased from Sigma-Aldrich in the purest commercially available grade and used as received. Water, with a resistivity of not less than 18 MΩ cm, was taken from an Elgastat system (Vivendi). Nitrogen and argon were obtained from Energas, Ltd, U.K..

Viscosities of dilute solutions were measured using an Ubbelohde viscometer mounted within a water bath thermostatted to 298 K. The viscometer was calibrated using pure water. Transmission electron microscopy was undertaken using a JEOL JEM1200EXII instrument equipped with energy-dispersive spectrometry (EDS) analysis (INCA Energy 350, Oxford Instruments). Images were acquired using a Gatan dual view camera.

Concentrated solutions and lyotropic liquid crystals were prepared by mixing the required mass of chlorpromazine hydrochloride with nitrogen- or argon-purged water in the appropriate wt % ratio in screw-capped vials sealed with Parafilm, followed by heating in a water bath, with stirring to approximately 363 K for 60 min, thereby achieving sample homogenization in the normal, isotropic micellar phase. The samples were then allowed to cool to ambient temperature (294 ± 2 K) prior to further experimentation at this temperature. Long-term (four months) exposure of the material to both oxygen and sunlight was undertaken through regular (weekly) opening of the sample vial to enable gas exchange, and keeping the glass vial containing the sample on a south-facing windowsill.

Concentrated samples were examined using an Olympus BX-51 optical polarizing microscope, equipped with a digital camera for image capture. Ultraviolet−visible spectrophotometry was undertaken using a PerkinElmer Lambda-25-Scan-UV−Vis instrument, using a quartz cell of 1.0 cm path length. X-ray scattering measurements were undertaken through filling capillary tubes with the viscous sample, placed into an MAR345 diffractometer with a two-dimensional (2D) image plate detector (Cu K_α radiation, graphite monochromator, λ = 1.54 Å, 130−300 mm detector-sample distance, with an exposure time of 30 min). The samples were heated (between 297 and 363 K) in the presence of a magnetic field using a home-built capillary furnace. The bulk electrical resistivity of the samples was measured using a CDM210 conductivity

https://dx.doi.org/10.1021/acsomega.0c05284
ACS Omega 2021, 6, 4630−4640

meter equipped with a four-pole CDC511T conductivity cell (Radiometer) inserted vertically into the sample. Rheological measurements were made using a Bohlin CVO 120 high-resolution rheometer in the controlled rate mode with a truncated cone (4° cone angle, 40 mm cone diameter) in plate geometry (200 μm gap width), at a temperature of 298 K. The lowest shear rate applied was 0.1 s^{-1}. For each step, shear was applied for ca. 10 s, during which the shear stress was measured and the viscosity of the material calculated. Measurements made where the deviation between the achieved and target shear rate was >5% were rejected.

Electrochemical experiments were undertaken using a variety of potentiostats (μAutolab Type III, or Autolab PGSTAT30, or a PalmSens Instrument). Cyclic voltammetry experiments employed a silver/silver chloride reference electrode (BAS), a nickel spiral or nichrome wire counter electrode, and a glassy carbon working electrode (of diameter 3.0 mm, BAS). In the case of dilute solutions, samples were not degassed prior to oxidative electrochemistry, but the working electrode was cleaned and polished using an aqueous 0.3 μm alumina slurry on a wetted, napped polishing cloth before every experiment so that a clean surface was exposed to different locations of the sample for every change in experimental variable. For voltammetric experiments within the redox liquid crystal, to overcome any effects due to wall slip, the phase was allowed to melt into the normal, isotropic micellar phase under argon, prior to insertion of the cleaned and polished 11.0 μm carbon microelectrode, together with the reference and counter electrodes. This system was then cooled to ambient temperature so that the insertion of the electrodes would not shear the liquid crystal. This procedure was repeated for every scan rate examined. For channel electrode measurements of dilute aqueous solutions, a bespoke, rectangular channel flow base plate (of length, L = 7 cm; width, d = 0.6 cm) was machined in PTFE using a CNC, covered with an optically pure silica cover plate (Optiglass, Ltd., Hainault, Essex, U.K.), and sealed with adhesive (Stick 2, Ever Build) so that the channel depth is $2h$ = 0.08 cm, where h is the half-cell depth. A platinum foil working electrode (of length, x_e = 0.55 cm, and width, w = 0.45 cm, measured accurately within a traveling microscope) was positioned so that its upstream edge was located two-thirds of the channel length downstream from the flow entrance. The platinum foil was connected via contact through the *verso* face with conductive epoxy through a hole at the bottom of the channel, and was polished using a cotton swab impregnated with 0.3 μm alumina slurry prior to sealing the channel flow cell. The long entry length (l_e) enabled the establishment of a laminar, Hagen−Poiseuille flow[85] ($l_e > 0.034hRe$, where Re is the Reynolds number, defined as $Re = d_e\hat{u}/\nu$, in which d_e is the hydraulic diameter, $d_e = 4hd/(2h + d)$, $\hat{u}$ is the free stream and average velocity, and ν is the kinematic viscosity), using a syringe pump (Fusion 200, CHEMYX) to drive the solution to flow between 5 and 50 μL s^{-1}, corresponding to $1.5 \leq Re \leq 15$. A saturated calomel reference (Radiometer) was positioned upstream to the channel flow cell, with a platinum mesh counter electrode placed downstream of the flow cell, so that the products formed on the counter electrode would not interfere with the process occurring on the working electrode during the recording of steady-state currents.

AUTHOR INFORMATION

Corresponding Author

Jay D. Wadhawan − *Department of Physical Sciences (Chemistry), University of Hull, Kingston-upon-Hull HU6 7RX, Humberside, United Kingdom;* orcid.org/0000-0002-1691-7169; Email: j.wadhawan@hull.ac.uk

Authors

Robert D. Crapnell − *Department of Physical Sciences (Chemistry), University of Hull, Kingston-upon-Hull HU6 7RX, Humberside, United Kingdom*

Huda S. Alhasan − *Department of Physical Sciences (Chemistry), University of Hull, Kingston-upon-Hull HU6 7RX, Humberside, United Kingdom*

Lee I. Partington − *Department of Physical Sciences (Chemistry), University of Hull, Kingston-upon-Hull HU6 7RX, Humberside, United Kingdom*

Yan Zhou − *Department of Physical Sciences (Chemistry), University of Hull, Kingston-upon-Hull HU6 7RX, Humberside, United Kingdom*

Ziauddin Ahmed − *Department of Physical Sciences (Chemistry), University of Hull, Kingston-upon-Hull HU6 7RX, Humberside, United Kingdom*

Amal A. Altalhi − *Department of Physical Sciences (Chemistry), University of Hull, Kingston-upon-Hull HU6 7RX, Humberside, United Kingdom*

Thomas S. Varley − *Department of Physical Sciences (Chemistry), University of Hull, Kingston-upon-Hull HU6 7RX, Humberside, United Kingdom*

Nadiyah Alahmadi − *Department of Physical Sciences (Chemistry), University of Hull, Kingston-upon-Hull HU6 7RX, Humberside, United Kingdom*

Georg H. Mehl − *Department of Chemistry, University of Hull, Kingston-upon-Hull HU6 7RX, United Kingdom;* orcid.org/0000-0002-2421-4869

Stephen M. Kelly − *Organic and Materials Chemistry, Department of Chemistry, Liquid Crystals and Organophotonics Research Group, University of Hull, Kingston-upon-Hull HU6 7RX, United Kingdom;* orcid.org/0000-0003-0668-6253

Nathan S. Lawrence − *Department of Physical Sciences (Chemistry), University of Hull, Kingston-upon-Hull HU6 7RX, Humberside, United Kingdom*

Frank Marken − *Department of Chemistry, University of Bath, Bath BA2 7AY, United Kingdom;* orcid.org/0000-0003-3177-4562

Complete contact information is available at: https://pubs.acs.org/10.1021/acsomega.0c05284

Notes

The authors declare no competing financial interest.

ACKNOWLEDGMENTS

The authors thank EPSRC (GR/N EP/G020833/1) and The University of Hull for financing this work. G.H.M. thanks EPSRC (GR/N EP/M015726/1) for funding. H.S.A. thanks the Iraqi Cultural Attache for financing her Ph.D. and The University of Babylon for further support. Y.Z. thanks China University of Petroleum for further funding. A.A.A. thanks the Royal Kingdom of Saudi Arabia for funding her Ph.D. and Taif University for further support. N.A. thanks The University of Jeddah for financial support. F.M. and J.D.W. thank Jon

https://dx.doi.org/10.1021/acsomega.0c05284
ACS Omega 2021, 6, 4630−4640

Mitchell (University of Bath) for undertaking TEM measurements. H.S.A. and J.D.W. thank Tim Dunstan (University of Hull) for undertaking rheological measurements. The contribution of Laurence Boulder, James Shellbourne, Laetita Testut, Håvard Eide, Haydn Ward, Adam Gregory, and Akalya Raviraj in repeating various aspects of this work is also acknowledged.

REFERENCES

(1) Evans, D. H.; O'Connell, K. M. Conformational Change and Isomerisation Associated with Electrode Reactions. In *Electroanalytical Chemistry*; Bard, A. J., Ed.; Marcel Dekker: New York, 1986; Vol. *14*, p 113.
(2) See, for example Pombeiro, A. J. L.; da Silva, M. F. C. G. Bond and Structure Activation by Anodic Electron Transfer: Metal-Hydrogen Bond Cleavage and *cis/trans* Isomerisation in Coordination Compounds. In *Trends in Molecular Electrochemistry*; Pombeiro, A. J. L.; Amatore, C., Eds.; Marcel Dekker: New York, 2004; p 153.
(3) Hale, J. M. The Rates of Reactions Involving Only Electron Transfer, at Metal Electrodes. In *Reactions of Molecules at Electrodes*; Hush, N. S., Ed.; John Wiley: London, 1971; p 229.
(4) Allendoerfer, R. D.; Reiger, P. H. Electrolytic reduction of cyclooctatetraene. *J. Am. Chem. Soc.* **1965**, *87*, 2336.
(5) Anderson, L. B.; Hansen, J. F.; Kakihana, T.; Paquette, L. A. Unsaturated heterocyclic systems part 74: electrochemical studies of reduction of 2-methoxyazocines in aprotic solvents − comparison with cyclooctatetraene system. *J. Am. Chem. Soc.* **1971**, *93*, 161.
(6) See, for example Savéant, J.-M. *Elements of Molecular and Biomolecular Electrochemistry*; John Wiley: Hoboken, NJ, USA, 2006.
(7) Amatore, C.; Maisonhaute, E.; Simonneau, G. Ohmic drop compensation in cyclic voltammetry at scan rates in the megavolt per second range: access to nanometric diffusion layers via transient electrochemistry. *J. Electroanal. Chem.* **2000**, *486*, 141.
(8) Amatore, C.; Maisonhaute, E.; Schöllhorn, B.; Wadhawan, J. Ultrafast voltammetry for probing interfacial electron transfer in molecular wires. *ChemPhysChem* **2007**, *8*, 1321.
(9) Moraczewski, J.; Geiger, W. E. Electrochemical properties of bis(cyclopentadienylcobalt)cyclooctatetraene: formation of 34-electron triple decker compound. *J. Am. Chem. Soc.* **1978**, *100*, 7429.
(10) Deschenaux, R.; Schweissguth, M.; Levelut, A.-M. Electron-transfer induced mesomorphism in the ferrocene-ferricenium redox system: the first ferricenium-containing thermotropic liquid crystal. *Chem. Commun.* **1996**, 1275.
(11) Deschenaux, R.; Schweissguth, M.; Vilches, M.-T.; Levelut, A.-M.; Hautot, D.; Long, G. J.; Luneau, D. Switchable mesomorphic materials based on the ferrocene-ferricenium redox system: electron transfer generated columnar liquid crystalline phases. *Organometallics* **1999**, *18*, 5553.
(12) Donnio, B.; Seddon, J. M.; Deschenaux, R. A ferrocene containing carbohydrate surfactant: thermotropic and lyotropic phase behaviour. *Organometallics* **2000**, *19*, 3077.
(13) Nakamura, Y.; Matsumoto, T.; Sakazume, Y.; Murata, J.; Chang, H.-C. Tuning the mesomorphism and redox response of anionic ligand-based mixed-valent nickel(II) complexes by alkyl-substituted quaternary ammonium cations. *Chem. - Eur. J.* **2018**, *24*, 7398.
(14) Bourdillon, C.; Demaille, C.; Moiroux, J.; Savéant, J.-M. New insights into the enzymatic catalysis of the oxidation of glucose by native and recombinant glucose oxidase mediated by electrochemically generated one-electron redox co-substrates. *J. Am. Chem. Soc.* **1993**, *115*, 1.
(15) Ban, T. A. Fifty years chlorpromazine: an historical perspective. *Neuropsychiatr. Dis. Treat.* **2007**, *3*, 495.
(16) See, for example Eckert, G. M.; Gutmann, F.; Keyzer, H. Electrochemistry of Drug Interactions and Incompatibilities. In *Modern Bioelectrochemistry*; Gutman, F.; Keyzer, H., Eds.; Plenum Press: New York, 1986; p 503.
(17) Dryhurst, G.; Kadish, K. M.; Scheller, F.; Renneberg, R. Phenothiazines. In *Biological Electrochemistry*; Academic Press: New York, 1982; Vol. *1*, p 180.
(18) Cheng, H. Y.; Sackett, P. H.; McCreery, R. L. Kinetics of chlorpromazine cation radical decomposition in aqueous buffers. *J. Am. Chem. Soc.* **1978**, *100*, 962.
(19) Cheng, H. Y.; Sackett, P. H.; McCreery, R. L. Reactions of chlorpromazine cation radical with physiologically occurring nucleophiles. *J. Med. Chem.* **1978**, *21*, 948.
(20) Deputy, A.; Wu, H.-P.; McCreery, R. L. Spatially resolved spectroelectrochemical examination of the oxidation of dopamine by chlorpromazine cation radical. *J. Phys. Chem. A* **1990**, *94*, 3620.
(21) Sackett, P. H.; Mayausky, J. S.; Smith, T.; Kalus, S.; McCreery, R. L. Side-chain effects on phenothiazine cation radical reactions. *J. Med. Chem.* **1981**, *24*, 1342.
(22) Bosch, E.; Kochi, J. K. Catalytic oxidation of chlorpromazine and related phenothiazines: cation radicals as the reactive intermediates in sulfoxide formation. *J. Chem. Soc., Perkin Trans. 1* **1995**, 1057.
(23) Ximenes, V. F.; Quaggio, G. B.; Graciani, F. S.; de Menezes, M. L. Oxidation of amino acids by chlorpromazine cation radical and co-catalysis by chlorpromazine. *Pharmacol. Pharm.* **2012**, *3*, 29.
(24) Rodrigues, T.; dos Santos, C. G.; Riposati, A.; Barbosa, L. R. S.; di Mascio, P.; Itri, R.; Baptista, M. S.; Nascimento, O. R.; Nantes, I. L. Photochemically generated stable cation radical of phenothiazine aggregates in mildly acid buffered solution. *J. Phys. Chem. B* **2006**, *110*, 12257.
(25) Ateş, S.; Somer, G. Photodegradation of chlorpromazine in aqueous solutions as studied by ultraviolet-visible spectrophotometry and voltammetry. *J. Chem. Soc., Faraday Trans. 1* **1981**, *77*, 859.
(26) Garcia, C.; Smith, G. A.; McGimpsey, W. G.; Kochevar, I. E.; Redmond, R. W. Mechanism and solvent dependence for photoionisation of promazine and chlorpromazine. *J. Am. Chem. Soc.* **1995**, *117*, 10871.
(27) Sarata, G.; Noda, Y.; Sakai, M.; Takahashi, H. Structure and dynamics of the lowest excited triplet states and cation radicals of phenothiazine and 2-chlorophenothiazine: transient resonance Raman and absorption study. *J. Mol. Struct.* **1997**, *413−414*, 49.
(28) Maruthamuthu, P.; Sharma, D. K.; Serpone, N. Sub-nanosecond relaxation dynamics of 2,2′-azinobis(3-ethylbenzothiazoline-6-sulfonate) and chlorpromazine: assessment of photosensitisation of a wide band gap metal oxide semiconductor TiO_2. *J. Phys. Chem. B* **1995**, *99*, 3636.
(29) Chignell, C. F.; Motten, A. G.; Buettner, G. R. Photoinduced free radicals from chlorpromazine and related phenothiazines: relationship to phenothiazine-induced photosensitisation. *Environ. Health Perspect.* **1985**, *64*, 103.
(30) Buettner, G. R.; Hall, R. D.; Chignell, C. F.; Motten, A. G. The stepwise biphotonic photoionisation of chlorpromazine as seen by laser flash photolysis. *Photochem. Photobiol.* **1989**, *49*, 249.
(31) Fenner, H.; Möckel, H. EPR spekten von radikalkationen aus promazin und chlorpomazin. *Tetrahedron Lett.* **1969**, 2815.
(32) Pan, D.; Shoute, L. C. T.; Phillips, D. L. Time-resolved resonance Raman and density functional study of the radical cation of chlorpromazine. *J. Phys. Chem. A* **2000**, *104*, 4140.
(33) Rupérez, F. L.; Conesa, J. C.; Soria, J.; Apreda, M. C.; Cano, F. H.; Foces-Foces, C. X-ray diffraction and electron paramagnetic resonance study of the chlorpromazine cation radical. *J. Phys. Chem. C* **1985**, *89*, 1178.
(34) Pan, D.; Phillips, D. L. Raman and density functional study of the S_0 state of phenothiazine and the radical cation of phenothiazine. *J. Phys. Chem. A* **1999**, *103*, 4737.
(35) Soltz, B. A.; Corey, J. Y.; Larsen, D. W. Molecular motion in chlorpromazine and chlorpromazine hydrochloride. *J. Phys. Chem. D* **1979**, *83*, 2162.
(36) Hough, E.; Hjorth, M.; Dahl, S. G. The structures of (dimethylaminopropyl)phenothiazine drugs and their metabolites, part II: chlorpromazine sulphoxide, $C_{17}H_{19}ClN_2OS$, at 120 K. *Acta Crystallogr., Sect. C: Cryst. Struct. Commun.* **1985**, *41*, 383.

https://dx.doi.org/10.1021/acsomega.0c05284
ACS Omega 2021, 6, 4630−4640

(37) McDowell, J. J. H. The crystal and molecular structure of chlorpromazine. *Acta Crystallogr., Sect. B: Struct. Crystallogr. Cryst. Chem.* **1969**, *25*, 2175.
(38) Ortiz, A.; Pardo, A.; Fernández-Alonso, J. I. Spectra of radical cations of phenothiazine derivatives in solution and solid state. *J. Pharm. Sci.* **1980**, *69*, 378.
(39) Bahnemann, D.; Asmus, K.-D.; Wilson, R. L. Free radical induced one-electron oxidation of the phenothiazines chlorpromazine and promethazine. *J. Chem. Soc., Perkin Trans 2* **1983**, 1661.
(40) Zhang, H.-M.; Ruan, X.-Q.; Guo, Q.-X.; Liu, Y.-C. A study on one-electron oxidation of phenothiazine derivatives by piperidine oxoammonium ion in SDS micelle. *Res. Chem. Intermed.* **1998**, *24*, 687.
(41) Domańska, U.; Pelczarska, A.; Pobudkowska, A. Solubility and pK_a determination of six structurally related phenothiazines. *Int. J. Pharm.* **2011**, *421*, 135.
(42) Attwood, D.; Boitard, E.; Dubès, J.-P.; Tachoire, H. Calorimetric study of the influence of electrolyte on the micellisation of phenothiazine drugs in aqueous solution. *J. Phys. Chem. B* **1997**, *101*, 9586.
(43) Attwood, D.; Natarjan, R. Micellar properties of chlorpromazine hydrochloride in concentrated electrolyte solutions. *J. Pharm. Pharmacol.* **1983**, *35*, 317.
(44) Attwood, D.; Mosquera, V.; Villar, V. P. Thermodynamic properties of amphiphilic drugs in aqueous solution. *J. Chem. Soc., Faraday Trans 1* **1989**, *85*, 3011.
(45) Attwood, D.; Waigh, R.; Blundell, R.; Bloor, D.; Thévand, A.; Boitard, E.; Dubès, J.-P.; Tachoire, H. ^1H and ^{13}C NMR studies of the self-association of chlorpromazine hydrochloride in aqueous solution. *Magn. Reson. Chem.* **1994**, *32*, 468.
(46) Pérez-Rodríguez, M.; Varela, L. M.; Taboada, P.; Attwood, D.; Mosquera, V. The temperature dependence of the micellisation of chlorpromazine hydrochloride in aqueous solution. *Colloid Polym. Sci.* **2000**, *278*, 706.
(47) Attwood, D.; Mosquera, V.; Novas, L.; Sarmiento, F. Micellisation in binary mixtures of amphiphilic drugs. *J. Colloid Interface Sci.* **1996**, *179*, 478.
(48) Attwood, D.; Florence, A. T.; Gillan, J. M. N. Micellar properties of drugs: properties of micellar aggregates of phenothiazines and their aqueous solutions. *J. Pharm. Sci.* **1974**, *63*, 988.
(49) Attwood, D.; Mosquera, V.; Rey, C.; Vasquez, E. Self-association of amphiphilic phenothiazine drugs in aqueous solutions of low ionic strength. *J. Chem. Soc., Faraday Trans.* **1991**, *87*, 2971.
(50) Attwood, D.; Dickinson, N. A.; Mosquera, V.; Villar, V. P. Osmotic and activity coefficients of amphiphilic drugs in aqueous solution. *J. Phys. Chem. E* **1987**, *91*, 4203.
(51) Ruso, J. M.; Attwood, D.; Taboada, P.; Suárez, M. J.; Sarmiento, F.; Mosquera, V. Activity and osmotic coefficients of promethazine and chlorpromazine hydrochlorides in aqueous solutions of low ionic strength. *J. Chem. Eng. Data* **1999**, *44*, 941.
(52) Perez-Villar, V.; Vazquez-Iglesias, M. E.; de Geyer, A. Small-angle neutron scattering studies of chlorpromazine micelles in aqueous solutions. *J. Phys. Chem. F* **1993**, *97*, 5149.
(53) Alam, M. S.; Naqvi, A. Z.; ud Din, K. Study of the cloud point of the phenothiazine drug chlorpromazine hydrochloride: effect of surfactants and polymers. *J. Dispersion Sci. Technol.* **2008**, *29*, 274.
(54) Dea, P. K.; Keyzer, H. Conformation and Electronic Aspects of Chlorpromazine in Solution. In *Modern Bioelectrochemistry*; Gutman, F.; Keyzer, H., Eds.; Plenum Press: New York, 1986; p 481.
(55) Atherton, A. D.; Barry, B. W. Micellar properties of phenothiazine drugs: a laser light scattering study. *J. Colloid Interface Sci.* **1985**, *106*, 479.
(56) Barbosa, L. R. S.; Caetano, W.; Itri, R.; de Mello, P. H.; Santiago, P. S.; Tabak, M. Interaction of phenothiazine compounds with zwitterionic lysophosphatidylcholine micelles: small angle X-ray scattering, electronic absorption spectroscopy and theoretical calculations. *J. Phys. Chem. B* **2006**, *110*, 13086.
(57) Numerous studies have reported the voltammetry or redox transformation of *N*-substituted phenothiazine derivatives, as given in references 58-67.
(58) Horn, J. J.; McCreedy, T.; Wadhawan, J. Amperometric measurement of gaseous hydrogen sulphide via a Clark-type approach. *Anal. Methods* **2010**, *2*, 1346.
(59) Huie, R. E.; Neta, P. Reaction of the vanadate ion with chlorpromazine and the chlorpromazine free radical with the vanadyl ion. *Inorg. Chim. Acta* **1984**, *93*, L27.
(60) Roseboom, H.; Perrin, J. H. Oxidation kinetics of phenothiazine and 10-methylphenothiazine in acidic medium. *J. Pharm. Sci.* **1977**, *66*, 1392.
(61) Karpińska, J.; Starczewska, B.; Puzanowska-Tarasiewicz, H. Analytical properties of 2- and 10-disubsituted phenothiazine derivatives. *Anal. Sci.* **1996**, *12*, 161.
(62) Cauquis, G.; Deronzier, A.; Lepage, J.-L.; Serve, D. Une nouvelle étude de l'oxydation électrochimique dy noyau phénothiazinique I: cas de la phénothiazine et de ses derives disubstitués en 3 et 7. *Bull. Soc. Chim. Fr.* **1977**, 295.
(63) Cauquis, G.; Deronzier, A.; Lepage, J.-L.; Serve, D. Une nouvelle étude de l'oxydation électrochimique dy noyau phénothiazinique II: cas de quelques biphénothiazinyles-1,10′ et −3,10′. *Bull. Soc. Chim. Fr.* **1977**, 303.
(64) Billon, J.-P. Etude électrochimique des propriétés oxydo-réductrices des phénothiazines dans l'acétonitrile. *Ann. Chim.* **1962**, *7*, 183.
(65) Humphry-Baker, R.; Braun, A. M.; Grätzel, M. Effect of self-assembly of amphiphilic redox chromophores on photoionisation processes. *Helv. Chim. Acta* **1981**, *64*, 2036.
(66) Grätzel, M. Interfacial Charge Transfer Reactions in Colloidal Dispersions and Their Application to Water Cleavage by Visible Light. In *Modern Aspects of Electrochemistry*; Plenum Press: New York, 1983; Vol. *15*, p 83.
(67) Krieg, M.; Pileni, M.-P.; Braun, A. M.; Grätzel, M. Micelle formation and surface activity of functional redox relays: viologens substituted by a long alkyl chain. *J. Colloid Interface Sci.* **1981**, *83*, 209.
(68) Rusling, J. F. Electrochemistry in Micelles and Microemulsions. In *Interfacial Kinetics and Mass Transport*; Calvo, E. J., Ed.; Wiley: Weinheim, 2003; Vol. *2*, p 418.
(69) See, for example Gooding, J. J.; Compton, R. G.; Brennan, C. M.; Atherton, J. H. A new electrochemical method for the investigation of the aggregation of dyes in solution. *Electroanalysis* **1997**, *9*, 759.
(70) Anicet, N.; Bourdillon, C.; Demaille, C.; Moiroux, J.; Savéant, J.-M. Catalysis of the electrochemical oxidation of glucose by glucose oxidase and a single electron co-substrate: kinetics in viscous solutions. *J. Electroanal. Chem.* **1996**, *410*, 199.
(71) Fahidy, T. Z. *Principles of Electrochemical Reactor Analysis*, Elsevier: Amsterdam, 1985.
(72) Halls, J. E.; Wadhawan, J. D. Photogalvanic cells based on lyotropic nanosystems: towards the use of liquid nanotechnology for personalised energy sources. *Energy Environ. Sci.* **2012**, *5*, 6541.
(73) Ekdawi, N.; Hunter, R. J. Couette flow behaviour of coagulated colloidal suspensions, part IV: the elastic floc model at low shear rates. *J. Colloid Interface Sci.* **1983**, *94*, 355.
(74) Bourgoin, D.; Shankland, W. Rheology of the lecithin-water system in its lamellar phase. *Rheol. Acta* **1980**, *19*, 226.
(75) Malkin, A. Y.; Patlazhan, S. A. Wall slip for complex liquids − phenomenon and its causes. *Adv. Colloid Interface Sci.* **2018**, *257*, 42.
(76) Binks, B. P.; Clint, J. H.; Whitby, C. P. Rheological behaviour of water-in-oil emulsions stabilised by hydrophobic bentonite particles. *Langmuir* **2005**, *21*, 5307.
(77) Evans, L. A.; Thomasson, M. J.; Kelly, S. M.; Wadhawan, J. Electrochemical determination of diffusion anisotropy in molecularly structured materials. *J. Phys. Chem. C* **2009**, *113*, 8901.
(78) Halls, J. E.; Lawrence, N. S.; Wadhawan, J. D. Electrochemical estimation of diffusion anisotropy of *N,N,N′,N′*-tetramethyl-*para*-phenylenediamine within the normal hexagonal lyotropic mesophase of Triton X 100/light water: when can the effects of cross-

https://dx.doi.org/10.1021/acsomega.0c05284
ACS Omega 2021, 6, 4630−4640

pseudophase electron transfer be neglected for partitioned reagents? *J. Phys. Chem. B* **2011**, *115*, 6509.
(79) Michael, A. C.; Wightman, R. M.; Amatore, C. A. Microdisc electrodes, part I: digital simulation with a conformal map. *J. Electroanal. Chem. Interfacial Electrochem.* **1989**, *267*, 33.
(80) Alden, J. A.; Hutchinson, F.; Compton, R. G. Can cyclic voltammetry at microdisc electrodes be approximately described by one-dimensional diffusion? *J. Phys. Chem. B* **1997**, *101*, 949.
(81) Savéant, J.-M.; Vianello, E. Potential-sweep voltammetry: general theory of chemical polarisation. *Electrochim. Acta* **1967**, *12*, 629.
(82) Ball, J. C.; Marken, F.; Fulian, Q.; Wadhawan, J. D.; Blythe, A. N.; Schröder, U.; Compton, R. G.; Bull, S. D.; Davies, S. G. Voltammetry of electroactive oil droplets, part II: comparison of experimental and simulation data for coupled ion and electron insertion processes and evidence for microscale convection. *Electroanalysis* **2000**, *12*, 1017.
(83) Nicholson, R. S.; Shain, I. Theory of stationary electrode polarography: single scan and cyclic methods applied to reversible, irreversible and kinetic systems. *Anal. Chem.* **1964**, *36*, 706.
(84) Cummings, C. Y.; Wadhawan, J. D.; Nakabayashi, T.; Haga, M.-A.; Rassaei, L.; Dale, S. E. C.; Bending, S.; Pumera, M.; Parker, S. C.; Marken, F. Electron hopping rate measurements in ITO junctions: charge diffusion in a layer-by-layer deposited ruthenium(II)-bis-(benzimidazolyl)pyridine-phosphonate-TiO_2 film. *J. Electroanal. Chem.* **2011**, *657*, 196.
(85) Wang, Y. L.; Longwell, P. A. Laminar flow in the inlet section of parallel plates. *AIChE J.* **1964**, *10*, 323.

https://dx.doi.org/10.1021/acsomega.0c05284
ACS Omega 2021, 6, 4630−4640